

Modern Physics Letters A
 © World Scientific Publishing Company

Probing Top Changing Neutral Higgs Couplings at Colliders

Wei-Shu Hou

Department of Physics, National Taiwan University, Taipei 10617, Taiwan
wshou@phys.ntu.edu.tw

Tanmoy Modak

Institut für Theoretische Physik, Universität Heidelberg, 69120 Heidelberg, Germany
tanmoyy@thphys.uni-heidelberg.de

Received (Day Month Year)

Revised (Day Month Year)

The $h(125)$ boson, discovered only in 2012, is lower than the top quark in mass, hence $t \rightarrow ch$ search commenced immediately thereafter, with current limits at the per mille level and improving. As the $t \rightarrow ch$ rate vanishes with the h - H mixing angle $\cos \gamma \rightarrow 0$, we briefly review the collider probes of the top changing tcH/tcA coupling ρ_{tc} of the exotic CP -even/odd Higgs bosons H/A . Together with an extra top conserving ttH/ttA coupling ρ_{tt} , one has an enhanced cbH^+ coupling alongside the familiar tbH^+ coupling, where H^+ is the charged Higgs boson. The main processes we advocate are $cg \rightarrow tH/A \rightarrow tt\bar{c}$, $tt\bar{t}$ (same-sign top and triple-top), and $cg \rightarrow bH^+ \rightarrow b\bar{t}b$. We also discuss some related processes such as $cg \rightarrow thh$, tZH that depend on $\cos \gamma$ being nonzero, comment briefly on $gg \rightarrow H/A \rightarrow t\bar{t}$, $t\bar{c}$ resonant production, and touch upon the ρ_{tu} coupling.

Keywords: extra top Yukawa couplings; exotic Higgs bosons; h - H mixing.

PACS Nos.: .

1. Introduction

It was proposed in the early 1990s, before the top quark was even discovered, that¹ “ $t \rightarrow ch$ or $h \rightarrow t\bar{c}$ decays could be quite prominent, if not the dominant, decay modes of the top quark and some neutral Higgs bosons” (h). The generic neutral Higgs boson h (whether scalar or pseudoscalar) in the two Higgs doublet model (2HDM) context can have $\bar{q}_i q_j h$ couplings proportional² to $\sqrt{m_i m_j}$, thereby evade effectively the low energy flavor changing neutral current (FCNC) constraints that so worried Glashow and Weinberg.³ As much as this Cheng-Sher ansatz² helped lead the way to identify tch as plausibly the largest flavor changing neutral Higgs (FCNH) coupling, it was pointed out¹ that $\sqrt{m_i m_j}$ dependence need not be literal,^a but just “reflect fermion mass and mixing hierarchies”, i.e. the flavor enigma. This

^aHall and Weinberg also discussed⁴ $t \rightarrow ch$ under approximate $U(1)$ flavor symmetries.

is distinct from the two usual 2HDMs, Models I and II, where the “Natural Flavor Conservation” (NFC) condition³ is enforced by a Z_2 symmetry that completely eliminates the second set of Yukawa couplings. The 2HDM with extra Yukawa couplings, i.e. without an *ad hoc* Z_2 symmetry, but controlled by the emergent and therefore “*natural*” fermion mass-mixing hierarchies, was christened¹ Model III. With the top quark nowhere to be seen at the time, it was even suggested⁵ that $m_t < M_W$ could still be possible, with $t \rightarrow bW^*$ obscured by e.g. $t \rightarrow ch$ (or bH^+). For a general review of 2HDMs, see Ref. 6.

But the top quark was discovered via the $t \rightarrow bW$ channel in 1995 at the Tevatron, while it took almost two more decades for the elusive $h(125)$ boson to be discovered at the Large Hadron Collider (LHC). To set up notation, we note the remarkable *emergent* phenomenon from LHC Run 1 data, called “alignment”: the $h(125)$ boson was found to resemble rather closely⁷ the Higgs boson of the Standard Model (SM). In the 2HDM framework, we denote $h(125)$ as h , while H/A and H^\pm are the exotic CP -even/odd and charged scalars, respectively.

After the top quark discovery,⁸ in context of the push (in the 1990s!) for a 500 GeV e^+e^- linear collider and other future facilities, top FCNH was studied for e^+e^- ,^{9–15} $\gamma\gamma$,¹⁶ and even¹⁷ $\mu^+\mu^-$ colliders. One novel idea was that $e^+e^- \rightarrow Z^* \rightarrow hA$ or HA pair production can¹⁰ give rise to $t\bar{t}\bar{c}$ final states,^b i.e. same-sign top production. Exotic scalar production by vector boson fusion with “neutrino tags”, i.e. the $e^+e^- \rightarrow t\bar{c}\nu_e\bar{\nu}_e$ process was also proposed,^{11–13} but this channel may not be promising, as the exotic scalars probably do not couple much with vector bosons due to alignment. The same-sign top idea, however, was carried over to the LHC, with the *direct* production process¹⁸ of $c\bar{g} \rightarrow tA$ followed by $A \rightarrow t\bar{c}$ decay, or $c\bar{g} \rightarrow t\bar{t}\bar{c}$. We will see that this process is still relevant, but we are getting ahead of ourselves.

Let us come back to the $t \rightarrow ch$ decay process. In SM, $t \rightarrow ch$ can only arise at the loop level^c hence *very* suppressed, i.e. at^{21,22} $\mathcal{B}(t \rightarrow ch) \sim 10^{-15}$ and even smaller for $t \rightarrow uh$. This is definitely out of reach,^d but it implies that any observation would indicate beyond SM (BSM) *New Physics*. Ref. 21 also discussed 2HDM II, but since the authors corrected a sign error for the SM result after Ref. 22 appeared, we do not quote their result. It was later found^{24,25} in 2HDM II that $\mathcal{B}(t \rightarrow ch) \sim 10^{-5}$ (or higher) can be reached, but this relies on large $\tan\beta$ enhancement, as is the study²⁶ of loop effects from a “2HDM for the top quark”.²⁷ A similar level can be reached in SUSY,²⁸ but it relies on flavor changing gluino couplings in a time far before the advent of the LHC. SUSY loop effects were of course followed up,²⁹ but became diminished³⁰ after $h(125)$ discovery. Other avenues explored are, to name a few, R -parity violation,³¹ quark singlets,^{32,33} warped extra dimensions,³⁴ mirror fermions,³⁵ composite Higgs,³⁶ and aligned 2HDM,³⁷ where the latter three are

^bThe conjugate process is always implied throughout the paper.

^cWe do not discuss loop-induced tcZ and $tc\gamma$ couplings as they are less promising in terms of rate. For an early exposition, we refer to Ref. 19, and references therein. A subsequent review can be found in Ref. 20, which covers different models and processes, including tree level effects.

^dThe much larger²³ $\mathcal{B}(t \rightarrow bW^*h) \simeq 2 \times 10^{-9}$ in SM is still out of reach.

post $h(125)$ discovery. None of these truly reach above 10^{-5} , hence all fall short of a theoretical sensitivity estimate³⁸ at $\sim 10^{-4}$ for the LHC.

In contrast to the above suppression of $t \rightarrow ch$ rates, the expectation in 2HDM III is wide open, as the process is tree level,^{1,39,40} which has also been studied via effective field theory (EFT).^{41–43} With the advent of the LHC, and with early indications of a light Higgs boson, a detailed study⁴⁴ advocated $t \rightarrow ch$ followed by $h \rightarrow b\bar{b}$ as the discovery mode. By the time the paper was published, however, ATLAS and CMS had discovered⁸ the $h(125)$ boson. It was then pointed out that $\mathcal{B}(t \rightarrow ch)$ at the percent level⁴⁵ was still possible, and the search began in earnest. Partially stimulated by the CMS hint⁴⁶ for $h \rightarrow \tau\mu$ decay from 8 TeV data, variants of 2HDM III were discussed,^{47–50} but soon died out when the hint was not confirmed by 13 TeV data.⁸ The experimental pursuits, however, continued.

There is actually a catch for $t \rightarrow ch$ search: the tch coupling is suppressed by h – H mixing, i.e. between the two CP -even bosons, hence nonobservation could be due to small mixing rather than small tcH coupling. In this Brief Review, we focus on probing top changing neutral Higgs (TCNH) couplings at colliders via *direct* production processes. Rather than 2HDM III, we shall call the 2HDM with extra Yukawa couplings “general 2HDM” (g2HDM). In what follows, we give our theoretical framework in Sec. 2, then discuss $t \rightarrow ch$ search in Sec. 3. We turn to our main theme of direct production processes via TCNH coupling in Sec. 4, where Sec. 4.1 covers the $cg \rightarrow tH/A \rightarrow t\bar{t}\bar{c}$, $t\bar{t}t$ processes, namely same-sign top with jet and the more exquisite triple-top, and Sec. 4.2 covers $cg \rightarrow bH^+ \rightarrow b\bar{t}\bar{b}$. In Sec. 5 we offer some discussion and cover a miscellany of topics, and present our summary and prospects in Sec. 6.

2. Theoretical Framework

It is useful to trace the theory development since the early days of the $t \rightarrow ch$ proposal.¹ The Cheng-Sher treatment, while evoking the mass-mixing hierarchy to evade low energy FCNC constraints, was somewhat vague regarding the Higgs bosons. The scenario does remove the usual but *ad hoc* Z_2 symmetry that enforces the NFC condition³ of Glashow and Weinberg, and more systematic works clarified⁵¹ the situation, both for the Higgs potential, and the Yukawa couplings.

We write the most general CP -conserving two Higgs doublet (without Z_2) potential in the Higgs basis as^{51,52}

$$V(\Phi, \Phi') = \mu_{11}^2 \Phi^2 + \mu_{22}^2 \Phi'^2 - (\mu_{12}^2 \Phi^\dagger \Phi' + \text{h.c.}) + \frac{\eta_1}{2} \Phi^4 + \frac{\eta_2}{2} \Phi'^4 + \eta_3 \Phi^2 \Phi'^2 + \eta_4 \Phi^\dagger \Phi'^2 + \left\{ \frac{\eta_5}{2} (\Phi^\dagger \Phi')^2 + [\eta_6 \Phi^2 + \eta_7 \Phi'^2] \Phi^\dagger \Phi' + \text{h.c.} \right\}. \quad (1)$$

where $\langle \Phi \rangle \neq 0$ by^e $\mu_{11}^2 = -\frac{1}{2}\eta_1 v^2$, while $\langle \Phi' \rangle = 0$ hence $\mu_{22}^2 > 0$. A second minimization condition, $\mu_{12}^2 = \frac{1}{2}\eta_6 v^2$, removes the soft μ_{12}^2 term, reducing the total number

^eWe note that, without a Z_2 symmetry, the usual notion of $\tan \beta = v_1/v_2$ is unphysical.⁵¹ Note also that the η_6 and η_7 terms in Eq. (1) would be absent in 2HDMs with Z_2 symmetry.

4 *W.-S. Hou and T. Modak*

of parameters to nine,⁵² with η_6 the sole parameter for h - H mixing, namely

$$M_{\text{even}}^2 = \begin{bmatrix} \eta_1 v^2 & \eta_6 v^2 \\ \eta_6 v^2 & m_A^2 + \eta_5 v^2 \end{bmatrix}, \quad (2)$$

for the CP -even Higgs mass matrix, where $m_A^2 = \mu_{22}^2 + \frac{1}{2}(\eta_3 + \eta_4 - \eta_5)v^2$. As mentioned, the *emergent* “alignment” phenomenon from LHC Run 1, that⁷ the h boson resembles rather closely the Higgs boson of SM, implies that the h - H mixing angle $\cos \gamma$ (which we denote as c_γ , and similarly $s_\gamma \equiv \sin \gamma$) is rather small. We note⁵² the approximate relation near alignment,

$$c_\gamma \cong \frac{\eta_6 v^2}{m_H^2 - m_h^2}, \quad (3)$$

as $s_\gamma \rightarrow 1$ more rapidly than $c_\gamma \rightarrow 0$. Thus, it is quite intuitive that Φ serves as the “mass-giver” with $\mu_{11}^2 < 0$, while Φ' is the exotic doublet with an inertial mass parameter $\mu_{22}^2 > 0$, and the “soft” μ_{12}^2 term is eliminated. This is in contrast to the usual 2HDM I and II with Z_2 symmetry, where both $m_{11}^2, m_{22}^2 < 0$, with the m_{12}^2 term playing the dual role of h - H mixing *and* inertial mass.

If one now takes the known $v \cong 246$ GeV as the sole scale parameter, then the traditional, elementary notion of “naturalness” dictates that all dimensionless quantities in $V(\Phi, \Phi')$, namely all η_i s and μ_{22}^2/v^2 in Eq. (1), ought to be $\mathcal{O}(1)$. It was shown explicitly in Ref. 52 (see Fig. 1 of the reference) that this “naturalness” can be maintained without running into conflict with alignment, i.e. c_γ in Eq. (3) can be small with large parameter space. Although $\eta_1 < \eta_6$ seems needed, both can be $\mathcal{O}(1)$, and the dynamical mixing parameter η_6 actually helps push $\eta_1 v^2$ down to the physical m_h^2 by level repulsion,^f hence μ_{11}^2/v^2 is indeed also $\mathcal{O}(1)$! This is in contrast even with SM, where the usual $\sqrt{\mu^2} \simeq 87$ GeV is a factor $\sim 2\sqrt{2}$ lower than v , which is borderline on being “natural”. Ref. 52 then asserts that, on top of mass-mixing hierarchy suppression in general,¹ the unforeseen emergent phenomenon of alignment, i.e. small c_γ , further suppresses the FCNH couplings of the lighter h . Thus, the combined effect of mass-mixing hierarchy and alignment can replace the brutal NFC condition, and one should therefore really view the usual Z_2 symmetry for what it is: *ad hoc*.

Though not spelled out in great detail in Ref. 52, the naturalness argument of $\mathcal{O}(1)$ parameters in $V(\Phi, \Phi')$, together with alignment, implies the mass range

$$m_H, m_A, m_{H^+} \in (300, 600) \text{ GeV}, \quad (4)$$

which seems just right for the LHC to probe. The point is, at the upper mass range and beyond, either one has $\eta_i > \mathcal{O}(1)$ (strong couplings), or $\mu_{22}^2/v^2 > \mathcal{O}(1)$ (decoupling) would set in. The former heads toward nonperturbativity, making estimates unreliable, while the latter would damp dynamical effects of interest. For the lower mass range, given that m_H^2 is raised by level repulsion, for $m_H < 300$ GeV or so

^fThe same level repulsion due to η_6 pushes $m_A^2 + \eta_5 v^2$ up to m_H^2 and helps maintain alignment.

would bring $m_A^2 + \eta_5 v^2$ closer to $\eta_1 v^2$, and even a weak η_6 could more easily generate c_γ , and alignment becomes harder to sustain. It should be clear that the sub-TeV range of Eq. (4) is just right for the LHC to probe in the next two decades.

Having accounted for the mass range of the exotic Higgs bosons, which is quite relevant for the LHC, we now write down^{51,53} the Yukawa couplings:^g

$$-\frac{1}{\sqrt{2}} \sum_{f=u,d,\ell} \bar{f}_i \left[(-\lambda_i^f \delta_{ij} s_\gamma + \rho_{ij}^f c_\gamma) h + (\lambda_i^f \delta_{ij} c_\gamma + \rho_{ij}^f s_\gamma) H - i \operatorname{sgn}(Q_f) \rho_{ij}^f A \right] R f_j - \bar{u}_i [(V \rho^d)_{ij} R - (\rho^{u\dagger} V)_{ij} L] d_j H^+ - \bar{\nu}_i \rho_{ij}^\ell R \ell_j H^+ + h.c., \quad (5)$$

where the generation indices i, j are summed over, $L, R = (1 \mp \gamma_5)/2$ are projection operators, and V is the Cabibbo-Kobayashi-Maskawa matrix, with the corresponding matrix in lepton sector taken as unity.^h The λ^f matrices have been diagonalized as usual with elements $\lambda_i^f = \sqrt{2} m_i^f / v$, but the extra Yukawa matrices, ρ^f , cannot be diagonalized simultaneously in principle. As has been said, however, the mass-mixing structure that Nature has revealed to us, together with the decoupling of h from ρ^f matrices in the alignment limit ($c_\gamma \rightarrow 0$), seem sufficient to shield FCNH couplings from our view, which could be the “flavor” design of Nature.

It should be stressed that, not only the ρ^f matrices cannot be simultaneously diagonalized with the λ^f matrices, they are in principle complex, with¹ ρ_{tc} and⁴⁵ ρ_{tt} expected to be the largest elements. In fact, ρ_{tt} being $\mathcal{O}(1)$ and complex is the most plausible, as it is the companion to the diagonal $\lambda_t \cong 1$, *which has been recently affirmed*^{55,56} *by experiment*. Exploiting this, it was shown that electroweak baryogenesis (EWBG) can be achieved,⁵⁷ with the CP violating (CPV) strength,

$$\lambda_t \operatorname{Im} \rho_{tt} = \mathcal{O}(1), \quad (6)$$

as the driver. Interestingly, the “naturalness” condition of $\mathcal{O}(1)$ dimensionless parameters in the Higgs potential is precisely what is needed to allow⁵⁸ a first order phase transition, a prerequisite for EWBG. On the other hand, with the recent order of magnitude improvement of the limit on the electron electric dipole moment (eEDM) by ACME18,⁵⁹ the EWBG study has been updated⁶⁰ by adding the previously ignored ρ_{ee} as a complex parameter. It is found that, so long that

$$\rho_{ee} / \rho_{tt} \propto \lambda_e / \lambda_t, \quad (7)$$

holds, which rhymes with the mass-mixing hierarchy, eEDM could be suppressed by two orders of magnitude or even more, and there can be an ACME (or other competing experiment) discovery in the not so distant future.

It can now be said that g2HDM touches “the Heavens and the Earth”! We now turn to see how extra Yukawa couplings can be explored at the LHC. We retrace in Sec. 3 the saga of the ongoing $t \rightarrow ch$ search, then on to our main theme of direct production processes via TCNH couplings in Sec. 4.

^gSimilar formulas were given in Ref. 54, but this reference assumed the ρ^f s are diagonal.

^hThis holds true as the active neutrinos are rather degenerate at vanishingly small masses.

3. Prelude: $t \rightarrow ch$ search

We have already given a brief survey of theory work on $t \rightarrow ch$ in the Introduction. But with $h(125)$ found lighter than top, one enters a different era. The searchⁱ for $t \rightarrow ch$ decay commenced immediately with the $h(125)$ discovery. Even if NFC is operative in Nature, it is a no-lose situation for pursuing the experimental search. It is in fact an obligation.

It should be clear that $\mathcal{B}(t \rightarrow ch)$ cannot be overly large, otherwise even Tevatron $t\bar{t}$ studies might have uncovered it. At the LHC, a multi-lepton analysis⁶¹ using CMS 7 TeV results⁶² gave a bound at 2.7% already in 2012. It was cautioned,⁴⁵ however, that one needs to take possible modifications of h properties into account. It was then⁴⁵ stressed that the $h(125)$ discovery events in ZZ^* final states themselves *could* contain information on $\mathcal{B}(t \rightarrow ch)$ because of its sizable branching fraction and exceptional cleanliness. For example, one should look for accompanying jets enriched with bs , if the events actually cascaded down from $t\bar{t}$ production. The conclusion was that 2011-2012 data should be able to reach the 1% level. This carried with it some sense of excitement, as discovery was possible. Indeed, the experimental measurements were already under way.

By 2013 summer conferences, ATLAS reported⁶³ a result on $t \rightarrow ch$ search via $h \rightarrow \gamma\gamma$ with 20 fb⁻¹ data at 8 TeV. The published limit⁶⁴ of 0.79% in 2014 at 95% C.L. indeed broke the 1% floor. Using same amount of data and combining $\gamma\gamma$ and multi-lepton results, CMS found⁶⁵ a better limit at 0.56%.

We refrain from accounting for further developments, as it is well documented in PDG,⁸ but comment that $t \rightarrow ch$ search via the dominant $h \rightarrow b\bar{b}$ decay has yet to deliver its full⁴⁴ promise, and should be explored further. The current best limit on $t \rightarrow ch$ search at 95% C.L. is from ATLAS,⁶⁶

$$\mathcal{B}(t \rightarrow ch) < 1.1 \times 10^{-3}, \quad (\text{ATLAS } 36 \text{ fb}^{-1}, 2019) \quad (8)$$

which combines the $h \rightarrow b\bar{b}$, $\tau\tau$ modes with earlier $h \rightarrow WW$, ZZ , and $\gamma\gamma$ Run 2 results. The two photon mode gave a limit⁶⁷ at 2.2×10^{-3} , but remarkably, the limit from the $\tau\tau$ mode⁶⁶ at 1.9×10^{-3} is better. As this is only a fraction of Run 2 data, the bound would continue to improve in the near future, while CMS should certainly be watched also.

Although experiments continue to set constraints on the effective λ_{tch} Yukawa coupling, Ref. 45 pointed out that the coupling in fact should be

$$\lambda_{tch} = \rho_{tc} c_\gamma, \quad (9)$$

in g2HDM, where ρ_{tc} is a TCNH coupling from the extra Yukawa matrix $\boldsymbol{\rho}^u$, defined in Eq. (5). Since we know that $c_\gamma \equiv \cos \gamma$ (denoted usually as $\cos(\beta - \alpha)$ in 2HDMs with Z_2) has to be small, the nonobservation so far can be accounted for, without

ⁱWe will keep to tch couplings in our main text, and comment on search for tuh couplings, where constraint is slightly weaker, in Sec. 5.

requiring ρ_{tc} to be small, even though discovery can still happen at any time.^j Note that we have dropped ρ_{ct} in Eq. (9), as it has to be rather small,⁵³ because its effect in B_d and B_s mixing is CKM enhanced.

4. Probing Extra Top Yukawa Couplings in Production Processes

From the emergent “alignment” phenomenon,⁷ we learned that Nature has further designs⁵² for suppressing FCNH effects at low energy: small c_γ , or alignment in the Higgs sector. This is reflected in Eq. (9), which can be read off from Eq. (5). It applies also to $h \rightarrow \tau\mu$, where there was once a hint⁸ from CMS Run 1 data, but not supported by Run 2 data (see footnote j below). To probe the TCNH coupling ρ_{tc} without c_γ suppression, one has to access the direct production of the H , A and H^+ bosons, where the mass range in Eq. (4) that follows from naturalness ($\mathcal{O}(1)$ parameters) seems tailor-made for the LHC. We turn to such processes, namely⁶⁸ $cg \rightarrow tH, tA$ and⁶⁹ $cg \rightarrow bH^+$, in this main section.

The existence of the extra diagonal Yukawa coupling ρ_{tt} means H, A can be produced by gluon-gluon fusion. We relegate resonance production, namely $gg \rightarrow H, A \rightarrow t\bar{t}, t\bar{c}$ and $\tau\mu$ to Sec. 5, as they face various and different challenges.

4.1. Top-associated H/A Production: $cg \rightarrow tH/tA \rightarrow t\bar{t}c, t\bar{t}\bar{c}$

We first consider $cg \rightarrow tH, tA$ production via the TCNH ρ_{tc} coupling (see Fig. 1), with subsequent decay of H, A to $t\bar{c}$ and $t\bar{t}$ final states, which depends on H, A masses and the strength of the extra diagonal ρ_{tt} coupling.

To compute the decay rates and parton cross sections, we simplify and take the alignment limit of $c_\gamma = 0$. The extra Yukawa couplings for u -type quarks are,

$$\frac{\rho_{ij}}{\sqrt{2}} \bar{u}_{iL}(H + iA)u_{jR} + \text{h.c.}, \quad (c_\gamma = 0) \quad (10)$$

where ρ_{ij} should share the “flavor organization” attributes of SM, i.e. trickling down off-diagonal elements. For sake of discussion, we keep only ρ_{tc} and ρ_{tt} finite (ρ_{ct} is constrained small⁵³ by B physics) and set all other ρ_{ij} s to zero, including those of down and lepton sectors, for the remainder of this section. For $S = H, A$, we

^jIn contrast, one does not quite expect $h \rightarrow \tau\mu$ to be seen, as the coupling $\rho_{\tau\mu}c_\gamma$ is suppressed by both $\rho_{\tau\mu} \lesssim \lambda_\tau \ll \rho_{tc}$ (most likely) as well as the alignment parameter c_γ . There was once a CMS hint from Run 1 data, but it subsequently disappeared by adding data.⁸

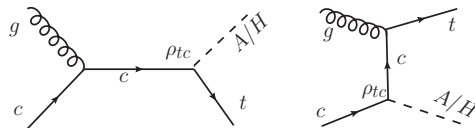


Fig. 1. The $cg \rightarrow tS$ ($S = H, A$) process.

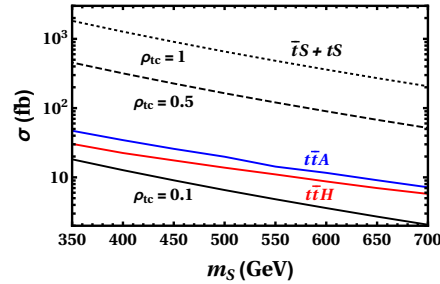


Fig. 2. Cross sections $\sigma(pp \rightarrow tS)$ and $\sigma(pp \rightarrow t\bar{t}S)$ for $\rho_{tt} = 1$ and $\rho_{tc} = 0.1$ (solid), 0.5 (dashed) and 1 (dots) at $\sqrt{s} = 14$ TeV.⁶⁸

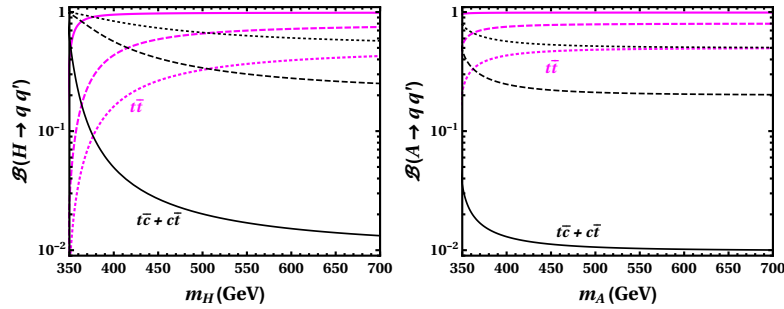


Fig. 3. $B(H/A \rightarrow t\bar{t}, t\bar{c})$ for $\rho_{tt} = 1$ and $\rho_{tc} = 0.1$ (solid), 0.5 (dashed) and 1 (dots).⁶⁸

display⁶⁸ $\sigma(cg \rightarrow tS)$ at parton level in Fig. 2 for $m_S \in (350, 700)$ GeV. The H, A decay branching fractions are given in Fig. 3.

We will see that⁶⁸ $cg \rightarrow tS \rightarrow t\bar{t}\bar{c}$, or same-sign top pair (SS2t) production,^k is already quite promising with 300 fb^{-1} if S is in the lower range of Eq. (4). For the higher mass range, i.e. S considerably above the $2m_t \gtrsim 350$ GeV threshold, the $t\bar{t}\bar{t}$ ($3t$) signature holds more promise in cutting down background at the High Luminosity LHC (HL-LHC). Note that the $3t$ cross section in SM is at $\mathcal{O}(\text{fb})$,⁷⁵ while g2HDM could enhance this by a factor of several hundred (cf. Fig. 2). Although both CMS⁷⁶ and ATLAS⁷⁷ have zoomed in on $t\bar{t}\bar{t}$ (i.e. $4t$) search¹ with full Run 2 data, neither experiments have initiated studies targeting $3t$ so far. We give in Fig. 2 also the $t\bar{t}S$ cross section, where $t\bar{t}A$ is larger than $t\bar{t}H$. While almost two orders below tS for $\rho_{tc} \simeq 1$, it can feed our signatures, and would dominate over tS for low ρ_{tc} .^m

^kSame-sign top was advocated⁷⁰ to appear with even 1 fb^{-1} LHC data due to some Tevatron “anomaly”, but this was quickly ruled out.^{71, 72} Same-sign top production has also been advocated recently with flavor-changing Z' ,^{73, 74} as well as neutral scalar ϕ exchange.⁷³

^lThis is in part because SM $4t$ cross section^{75, 78} at $\sim 12 \text{ fb}$ is an order of magnitude larger than $3t$ in SM, hence can be measured sooner if SM holds true.

^mWe do not include⁷⁹ $t\bar{c}S$ in Fig. 2. However, it is included in our collider signal for the inclusive same-sign top (marked as SS2t) production discussed in Sec. 4.1.2.

4.1.1. Collider Constraints on ρ_{tc}

A small c_γ makes the $t \rightarrow ch$ constraint on ρ_{tc} rather mute. But since the original proposal⁶⁸ for $cg \rightarrow tH/tA \rightarrow tt\bar{c}$ search, both CMS⁷⁶ and ATLAS⁷⁷ have now searched for $4t$ production with full Run 2 data set of 137 fb^{-1} at 13 TeV. Some of the Control Regions (CRs) of these $4t$ studies can probe into the $SS2t$ signature, which can be used to constrain ρ_{tc} , independent of c_γ . The results of this and the following subsection therefore follow the more recent analysis of Ref. 80, updating from Ref. 68 for the ρ_{tc} study.

Let us start with the CMS $4t$ search.⁷⁶ With the baseline selection criterion of at least two same-sign leptons, we find the most stringent constraint on ρ_{tc} arises from CRW,⁷⁶ the CR of ttW . The CRW of the CMS $4t$ search⁷⁶ is defined as containing two same-sign leptons plus two to five jets with two b -tagged. The selection cuts are as follows. For leading (subleading) lepton transverse momentum, $p_T^{\ell_1(\ell_2)} > 25(20) \text{ GeV}$. For pseudorapidity, $\eta^e < 2.5$ while $\eta^{\mu,j} < 2.4$. The p_T of (b -)jets should satisfy one of the following: (i) $p_T > 40 \text{ GeV}$ for both b -jets; (ii) $p_T > 20 \text{ GeV}$ for one b -jet, $20 < p_T < 40 \text{ GeV}$ for the second b -jet, and $p_T > 40 \text{ GeV}$ for the third jet; (iii) $20 < p_T < 40 \text{ GeV}$ for both b -jets, with two extra jets each satisfying $p_T > 40 \text{ GeV}$. Defined as the scalar sum of p_T of all jets, one requires $H_T > 300 \text{ GeV}$, while $p_T^{\text{miss}} > 50 \text{ GeV}$. To reduce the Drell-Yan background with a charge-misidentified (Q -flip) electron, events with same-sign electron pairs with $m_{ee} < 12 \text{ GeV}$ are rejected. Using these selection cuts, CMS reports 338 observed events in CRW, with 335 ± 18 events (SM backgrounds plus $4t$) expected.⁷⁶

To estimate our limits, we use MadGraph5_aMC@NLO⁸¹ (denoted as MadGraph5_aMC) to generate signal events for $\sqrt{s} = 13 \text{ TeV}$ at leading order (LO) with default parton distribution function (PDF) set NN23LO1,⁸² interface with PYTHIA 6.4⁸³ for showering and hadronization, and MLM matching^{84,85} prescription for matrix element (ME) and parton shower merging. The event samples are then fed into DELPHES 3.4.2⁸⁶ for fast detector simulation. We utilize the default b -tagging efficiency and light-jet rejection of DELPHES CMS-based detector card. The jets are reconstructed via anti- k_T algorithm with radius parameter $R = 0.6$, whereas the effective model is implemented in FeynRules.⁸⁷

The $pp \rightarrow tH/tA \rightarrow tt\bar{c}$ process with both top quarks decaying semileptonically (nonresonant $cg \rightarrow tt\bar{c}$, t -channel H/A exchange $cc \rightarrow tt$ and $gg \rightarrow t\bar{c}A/H$ processes are included) contributes to CRW of the CMS $4t$ search. Setting all other $\rho_{ij} = 0$, we estimate the cross section for $\rho_{tc} = 1$ then scale by ρ_{tc}^2 , assuming narrow H/A widths with $\mathcal{B}(H/A \rightarrow t\bar{c} + \bar{t}c) = 100\%$. We then demand the sum of expected SM and ρ_{tc} -induced events agree with observed, where the 2σ excluded region from CRW is displayed in Fig. 4[left] in purple, assuming Gaussian behavior for simplicity. To avoid cancellation⁶⁸ between H and A mediated production processes, we have assumed a splitting of $m_A - m_H = 50 \text{ GeV}$. This almost doubles the production rate, while if one of the exotic boson is much heavier than the other, the cross section drops by roughly one half. One can see the power of the $4t$ search, constraining ρ_{tc}

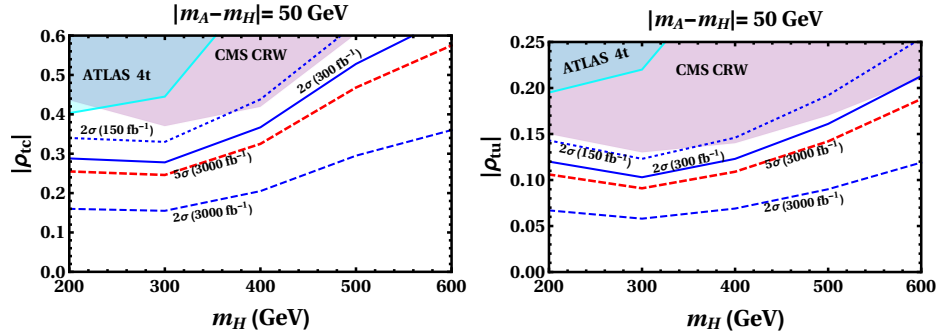


Fig. 4. [left] Constraint from $4t$ search in m_H - ρ_{tc} plane (with $m_A - m_H = 50$ GeV) by CRW of CMS⁷⁶ (purple) and CRttW2 ℓ of ATLAS⁷⁷ (cyan), setting all other $\rho_{ij} = 0$. Plotted further are the exclusion limits (blue) and discovery reaches (red) for ρ_{tc} from same-sign top signature for various integrated luminosities at the 14 TeV LHC. [right] The same for ρ_{tu} .⁸⁰

especially for m_S not far above the $t\bar{t}$ threshold of 350 GeV, but tapers off rapidly for heavier Higgs bosons due to rapid fall in the parton luminosity.

ATLAS has also searched for $4t$ production⁷⁷ with 139 fb^{-1} , but categorizing into different CRs and Signal Regions (SRs). Again the CR for $t\bar{t}W$, called CRttW2 ℓ , is the most relevant. It is defined as at least two same-sign leptons ($e\mu$ or $\mu\mu$), plus at least four jets with at least two b -tagged, where $p_T > 28$ GeV with $\eta^\mu < 2.5$ and $\eta^e < 1.5$ for the same-sign leptons. All jets should satisfy $p_T > 25$ GeV and $\eta < 2.5$. For two b -jets, or three or more b -jets but with no more than 5 jets, the scalar p_T sum over all jets and same-sign leptons (different from CMS), $H_T < 500$ GeV. Unlike CRW for CMS, ATLAS does not give the observed number of events in CRttW2 ℓ , but provides a figure of comparison between data and prediction in the variable $\sum p_T^\ell$ (see Ref. 77 for definition). We follow Ref. 88 and digitize the figure to extract the number of expected and observed events in the CRttW2 ℓ from the $\sum p_T^\ell$ distribution. We find 378 ± 10 and 380, respectively, where we simply add the errors in quadrature for the expected events from each $\sum p_T^\ell$ bin.

To extract the constraint, we follow the event selection as described and use now the ATLAS-based detector card of DELPHES. Assuming that the ρ_{tc} -induced events plus SM stay within 2σ of expected, the exclusion limits from ATLAS are the cyan shaded region in Fig. 4[left], which is weaker due to different selection cuts. From CMS $4t$ search, we find $\rho_{tc} \lesssim 0.37$ – 0.44 is still allowed for $200 \text{ GeV} \lesssim m_H \lesssim 400 \text{ GeV}$, while larger values open up quickly for $m_H > 400 \text{ GeV}$. We again illustrate for $m_H - m_A = 50 \text{ GeV}$, as there is strong cancellation⁶⁸ between $cg \rightarrow tH \rightarrow t\bar{t}\bar{c}$ and $cg \rightarrow tA \rightarrow t\bar{t}\bar{c}$ amplitudes for H, A that are nearly degenerate in mass and width. Note also that SUSY and other exotic searches nowadays use rather strong cuts and do not give relevant constraints for our relatively low mass range.

Fig. 4[right] is done in the same way as the left-hand plot, but with ρ_{tc} replaced⁸⁰ by ρ_{tu} , which we would discuss only in Sec. 5.

4.1.2. Same-sign Top: $cg \rightarrow tH/tA \rightarrow tt\bar{c}$

Although existing $4t$ searches with full LHC Run 2 data can constrain ρ_{tc} , they are not optimized for $cg \rightarrow tH/tA \rightarrow tt\bar{c}$ search. We advocate⁶⁸ a dedicated study of a stand-alone ρ_{tc} coupling with all other $\rho_{ij} = 0$.

The $pp \rightarrow tH/tA + X \rightarrow tt\bar{c} + X$ signature is defined as same-sign dilepton (ee , $e\mu$, $\mu\mu$) plus at least three jets with at least two b -tagged and one non- b -tagged, and E_T^{miss} . The SM backgrounds are $t\bar{t}Z$, $t\bar{t}W$, $4t$, $t\bar{t}h$, with tZ +jets subdominant ($3t+j$ and $3t+W$ turn out negligible). The $t\bar{t}$ and $Z/\gamma^* + \text{jets}$ processes, with sizable cross sections, would contribute if one lepton charge is misidentified (Q -flip), with probability taken as^{89–91} 2.2×10^{-4} in our analysis.

As before, we generate signal and background events at LO via MadGraph5_aMC but for $\sqrt{s} = 14$ TeV and follow the same showering, hadronization, ME matching and parton shower merging, but adopt the default ATLAS-based detector card of DELPHES. The LO $t\bar{t}W^-$ ($t\bar{t}W^+$), $t\bar{t}Z$, $4t$, $t\bar{t}h$ and tZ +jets cross sections are normalized to next-to-leading order (NLO) K factors 1.35 (1.27),⁹² 1.56,⁹³ 2.04,⁸¹ 1.27,⁹⁴ and 1.44⁸¹ respectively. We assume the same K factor for tZ +jets background for simplicity. The Q -flip $t\bar{t}$ +jets and $Z/\gamma^* + \text{jets}$ backgrounds are corrected to NNLO cross sections by 1.27⁹⁵ and 1.84,⁹⁶ respectively, where we use FEWZ 3.1⁹⁷ to obtain the latter factor for $Z/\gamma^* + \text{jets}$.

To suppress backgrounds and optimize for $pp \rightarrow tA/tH + X \rightarrow tt\bar{c} + X$, we take a cut based analysis that differs from CRW of CMS $4t$ search. For leading (subleading) lepton, $p_T^{\ell_1(\ell_2)} > 25$ (20) GeV, while $\eta^{\ell_1, \ell_2} < 2.5$. For all three jets, $p_T > 20$ GeV and $\eta < 2.5$, and we demand $E_T^{\text{miss}} > 30$ GeV. The separation ΔR between (i) a lepton and any jets ($\Delta R_{\ell j}$), (ii) the two b -jets (ΔR_{bb}), and (iii) any two leptons ($\Delta R_{\ell\ell}$) should all satisfy $\Delta R > 0.4$. Finally, with ATLAS definition of H_T , i.e. with p_T of the two leading leptons included, we demand $H_T > 300$ GeV. The signal cross sections for select m_H values are given in the first column of Table 1, together with the estimated background cross sections, where the K factors from LO to NLO are shown in brackets. There are also “nonprompt” backgrounds. The CMS study of same-sign dilepton (SS2 ℓ) signature,⁹⁸ with slightly different cuts than ours, finds nonprompt background at ~ 1.5 times the $t\bar{t}W$ background. These backgrounds are not properly modeled in our Monte Carlo simulations, and we simply add such backgrounds to the overall background at 1.5 times $t\bar{t}W$ after selection cuts. A realistic analysis by the experiments can handle this better.

To estimate the exclusion limit (2σ) and discovery potential (5σ), we utilize the test statistics⁹⁹

$$Z(nx) = \sqrt{-2 \ln \frac{L(nx)}{L(nn)}}, \quad (11)$$

where $L(nx) = e^{-x} x^n / n!$ is the likelihood function of Poisson probabilities with n the observed number of events, and x is either the number of events predicted by the background-only hypothesis b , or signal plus background hypothesis $s + b$. For

Table 1. The signal cross sections of the same-sign top SS2 t after selection cuts for different m_H (in parentheses) with $m_A = m_H + 50$ GeV for $\rho_{tc} = 1$ at 14 TeV LHC. Various backgrounds cross sections after selection cuts are presented in the third column, where numbers in brackets in second column are LO to NLO K factors.

Signal cross section in fb (m_H in GeV)	Backgrounds	Cross section (fb)
3.83 (200)	$t\bar{t}W$ [1.35 (1.27)]	1.31
4.12 (300)	$t\bar{t}Z$ [1.56]	1.97
2.35 (400)	$4t$ [2.04]	0.092
1.14 (500)	$t\bar{t}h$ [1.27]	0.058
0.75 (600)	Q -flip [1.84/1.27]	0.024
	tZ +jets [1.44]	0.007

exclusion ($s + b$) hypothesis, we demand $Z(bs + b) \geq 2$ for 2σ , while for discovery (b hypothesis), we demand $Z(s + bb) \geq 5$ for 5σ . The signal cross sections for the reference $\rho_{tc} = 1$ value after selection cuts are given in Table 1 for several m_H values with $m_A - m_H = 50$ GeV, assuming $m_H > m_A$. Utilizing the signal and background cross sections in Table 1, we present in Fig. 4[left] the exclusion and discovery contours by scaling the signal cross section with $\rho_{tc}^2 \mathcal{B}(A/H \rightarrow t\bar{c} + \bar{t}c)$ in m_H - ρ_{tc} plane for different luminosities. We set all $\rho_{ij} = 0$ in generating signal, which simply translates to $\mathcal{B}(A/H \rightarrow t\bar{c} + \bar{t}c) = 100\%$. We repeat a similar analysis with stand-alone ρ_{tu} (all other $\rho_{ij} = 0$) replacing ρ_{tc} , i.e. for the $pp \rightarrow tA/tH + X \rightarrow tt\bar{u} + X$ process induced by the $ug \rightarrow tH/tA \rightarrow tt\bar{u}$ at parton level. The exclusion limits and discovery potential are plotted in Fig. 4[right]. In Fig. 4, we have simply interpolated the contours from m_H values given in Table 1, and analogously for ρ_{tu} case.

We see from Fig. 4[left] that CRW of CMS $4t$ search⁷⁶ is suitably powerful: with full Run 2 data, our target analysis can only probe the region of $\rho_{tc} \sim 0.34$ – 0.4 , while adding full Run 3 data, the sensitivity extends to a broader region of parameter space, but so would the continued $4t$ analysis. The 5σ discovery region for 3000 fb^{-1} is somewhat better than the 300 fb^{-1} exclusion limit, and one can follow up on any hint from full Run 2+3 data. To be watched is $\rho_{tc} \sim 1$, needed for the backup mechanism for EWBG,⁵⁷ for $m_{H,A}$ at the higher end of the mass range in Fig. 4[left]. The high significance found in Ref. 68 suggests it could already be relevant in LHC Run 2. Same-sign top pair search has the potential to reveal to us whether the $\rho_{tc} \sim 1$ mechanism for EWBG is allowed.

As noted, CMS has searched⁹⁸ for SS2 ℓ events using $\sim 36 \text{ fb}^{-1}$ data at 13 TeV, which can constrain ρ_{tc} . It is found⁶⁸ that the constraint is only $\rho_{tc} \gtrsim 1$ for $S = H, A$ at 350 GeV, and tapers off to higher values, so does not affect our discussion above. The CMS update¹⁰⁰ with full Run 2 data does not change this conclusion, as cuts have moved upward hence missing our target mass range.

4.1.3. Triple-Top: $cg \rightarrow tH/A \rightarrow t\bar{t}$

We would advocate,⁶⁸ however, that “triple-top” search is more informative with a larger dataset. New physics triple-top search has been advocated in topcolor-assisted technicolor model,¹⁰¹ usual 2HDM with Z_2 symmetry,^{102,103} a literal effective tqh coupling,^{104,105} flavor-changing Z' ,⁷⁴ and also using EFT approach with four-fermi operators involving triple-top.^{106–108} Our sub-TeV exotic Higgs bosons have dimension-4 couplings (Sec. 2) that render an EFT approach artificial.

As $S \rightarrow t\bar{t}$ decay is needed for $cg \rightarrow tS$ to contribute, it is less sensitive just above $t\bar{t}$ threshold. With cross sections smaller due to more exquisite selection cuts, we give results for 3000 fb^{-1} . Unlike Sec. 4.1.2 for $SS2t$, the result presented here have not been updated to take sufficient account of $4t$ constraint with full Run 2 data. In this subsection, we take $\rho_{tt} = 1$.

We denote our triple-top signature as $3\ell 3b$, which is defined as: at least three leptons, at least three jets with at least three tagged as b -jets, plus E_T^{miss} . The selection cuts are: for the three leading leptons and b -jets, $p_T^\ell > 25 \text{ GeV}$ and $p_T^b > 20 \text{ GeV}$, respectively; η , ΔR and E_T^{miss} are the same as for $SS2t$; scalar sum, H_T , of transverse momenta of all three leading leptons and b -jets should satisfy $H_T > 320 \text{ GeV}$. To reduce $t\bar{t}Z + \text{jets}$ background, we veto¹⁰⁹ the mass range $76 \text{ GeV} < m_{\ell\ell} < 95 \text{ GeV}$ for same flavor, opposite charged lepton pairs, and if more than one pair is present, the veto is applied to the pair mass closest to m_Z .

Dominant SM backgrounds are $t\bar{t}Z + \text{jets}$ and $4t$, with $t\bar{t}W + \text{jets}$, $t\bar{t}h$ and $tZ + \text{jets}$ subdominant ($3t + j$, $3t + W$ are less than subdominant). The $t\bar{t} + \text{jets}$ process can contribute if a jet gets misidentified as a lepton, with probability taken as^{90,110} $\epsilon_{\text{fake}} = 10^{-4}$. We do not include nonprompt backgrounds as they are not properly modeled in Monte Carlo simulations. Unlike the $SS2t$ signature, the three hard leptons plus high b -jet multiplicity, along with Z -pole veto and H_T cut may reduce such contributions significantly. The $t\bar{t}Z + \text{jets}$, $4t$, $t\bar{t}W + \text{jets}$, $t\bar{t}h$ and $tZ + \text{jets}$ cross sections at LO are adjusted by the same factors as for $SS2t$, i.e. 1.56, 2.04, 1.35, 1.27 and 1.44 respectively, and likewise 1.84 for $t\bar{t} + \text{jets}$ with jet faking lepton. Conjugate processes are assumed to have the same correction factors for simplicity.

With background cross sections given in Table 2, the signal cross sections after

Table 2. Backgrounds for $3\ell 3b$ process at 14 TeV, where LO to NLO K -factors (cross sections with Z -pole veto) are given in the first (second) parentheses.⁶⁸

Backgrounds	Cross section (fb)
$t\bar{t}Z + \text{jets}$ (1.56)	0.0205 (0.0026)
$4t$ (2.04)	0.0232 (0.0209)
$t\bar{t}W + \text{jets}$ (1.35)	0.0017 (0.0015)
$t\bar{t}h$ (1.27)	0.0015 (0.0013)
$tZj + \text{jets}$ (1.44)	0.0002 (–)
$t\bar{t} + \text{jets}$ (fake)	0.0026 (0.0025)

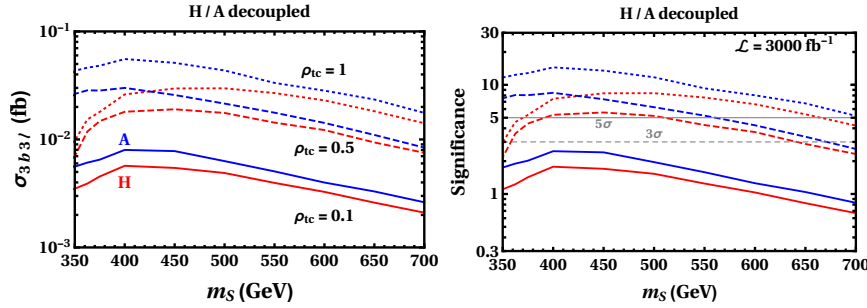


Fig. 5. [left] Cross sections (fb), and [right] significance (at 3000 fb^{-1}) for $3\ell 3b$ final state at $\sqrt{s} = 14 \text{ TeV}$ for $\rho_{tt} = 1$ and several ρ_{tc} values after selection cuts.⁶⁸

selection cuts are plotted in Fig. 5[left] for $\rho_{tt} = 1$ and $\rho_{tc} = 0.1, 0.5$ and 1 . For $\rho_{tc} = 1$ and 0.5 , $\mathcal{B}(A \rightarrow t\bar{t}) > \mathcal{B}(H \rightarrow t\bar{t})$ (see Fig. 3) makes the cross section for A higher than H , which also explains the slower turn on for H with m_H . For $\rho_{tc} = 0.1$, the $t\bar{t}S$ process dominates, with higher cross section for A (see Fig. 2). The discovery contours, estimated using Eq. (11) for 3000 fb^{-1} , are plotted in Fig. 5[right]. We find 5σ discovery reach for $\rho_{tc} = 1$ covers the full range of Eq. (4) and even a bit beyond. For $\rho_{tc} = 0.5$, 5σ reach is up to 520 (570) GeV for H (A) while 3σ evidence covers the full range of Eq. (4). With no interference between A and H induced contributions for triple-top, a small A - H mass splitting makes little effect, hence⁶⁸ for degenerate A - H , one could make 5σ discovery even beyond the full range of Eq. (4).

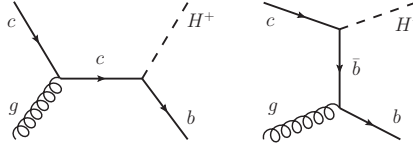
For lower masses with small splitting, the relative strength of triple-top and same-sign top at HL-LHC could in principle allow one to extract information on relative strength of ρ_{tc} vs ρ_{tt} , assuming discovery.⁶⁸ This would throw light on whether EWBG is more driven by ρ_{tt} or ρ_{tc} . Although we have elucidated the effect of exotic H and A scalars, mass reconstruction would not be easy, and further study would be needed, especially at HL-LHC.

We have assumed nearly degenerate heavy scalars, which need not be the case. Finite splittings could lead to $H \rightarrow AZ$, $H^\pm W^\mp$ (or reverse) decays, which would dilute our signatures but enrich the program. One charming aspect of extra ρ_{tt} and ρ_{tc} Yukawa couplings is their intrinsic complexity, which is why they can drive EWBG.⁵⁷ More studies are needed to probe these CPV phases. Our proposal is thus only a first step of a large program.

4.2. Bottom-associated H^+ Production: $cg \rightarrow bH^+ \rightarrow b\bar{t}\bar{b}$

A novel process, $cg \rightarrow bH^+$ (see Fig. 6) followed by $H^+ \rightarrow t\bar{b}$, was proposed recently,⁶⁹ that may lead to the discovery of the exotic H^+ boson in the near future.

The usual 2HDM II motivates the study of the $\bar{b}g \rightarrow \bar{t}H^+$ process^{111,112} which goes through the $\bar{t}bH^+$ coupling. In contrast, despite being phase space favored, the $cg \rightarrow bH^+$ process is suppressed by the Cabibbo-Kobayashi-Maskawa (CKM) matrix element ratio $V_{cb}/V_{tb}^2 \sim 1.6 \times 10^{-3}$. But in g2HDM with *extra* Yukawa

Fig. 6. Feynman diagrams for $cg \rightarrow bH^+$.

couplings,ⁿ $\bar{c}bH^+$ and $\bar{t}bH^+$ couple with strength⁶⁹ $\rho_{tc}V_{tb}$ and $\rho_{tt}V_{tb}$, respectively, and $cg \rightarrow bH^+$ is *not* CKM-suppressed. Although this fact can be read off from the H^+ coupling in Eq. (5), it is not quite “apparent”, and was realized after a study¹¹⁸ of H^+ effect in $B \rightarrow \mu\bar{\nu}$. We turn to the $cg \rightarrow bH^+ \rightarrow b\bar{t}$ process in this section. The process was noted by others,^{79,119,120} but were either mentioned without collider study, or without sufficient detail. For example, the $gg \rightarrow \bar{c}bH^+$ process was discussed in Ref. 79, but Fig. 6[left] was not explicitly mentioned, and in absence of a detailed collider study, the promise was not quite elucidated.

4.2.1. Constraints on Higgs and Flavor Parameters

We express^{51,52} the quartic couplings η_1, η_{3-6} in terms of μ_{22}, m_{h,H,A,H^+} (which are all normalized to v) and $\cos\gamma$, plus η_2, η_7 that do not enter Higgs masses. As Yukawa couplings of H^+ do not depend on c_γ , which is known to be small, we set $c_\gamma = 0$ (thus, e.g. $t \rightarrow ch$ does not constrain ρ_{tc}) while fixing $m_h \cong 125$ GeV. Thus,⁵² $\eta_6 = 0$ and $\eta_1 = m_h^2/v^2$, which simplifies the study considerably. In the Higgs basis, we identify η_{1-7} with the input parameters Λ_{1-7} to 2HDMC,¹²¹ which we utilize to check they satisfy positivity, perturbativity and tree-level unitarity.

For fixed $m_{H^+} = 300$ and 500 GeV, we randomly generate the parameters in the ranges $\eta_{2-5,7} \leq 3$ (except $\eta_2 > 0$ by positivity), $\mu_{22} \in [0, 1]$ TeV, and $m_{A,H} \in [m_{H^+} - m_W, 650$ GeV] to forbid $H^+ \rightarrow AW^+, HW^+$, again to simplify. The generated parameters are passed to 2HDMC for scanning, where we follow the scanning procedure discussed in Ref. 125. We further impose the electroweak oblique parameter constraints,¹²² which restricts^{123,124} the scalar masses hence the η_i s. Scan points satisfying these constraints⁶⁹ are plotted in Fig. 7 in the m_H – m_A plane for $m_{H^+} = 300, 500$ GeV, which illustrates that finite parameter space exist. We choose a benchmark for each m_{H^+} value and list the parameters in Table 3.

Flavor Constraints

With large parameter space for the Higgs sector demonstrated, we turn to flavor and collider constraints on ρ_{tc} and ρ_{tt} . Flavor constraints are not very strong.^{45,53} For $m_{H^+} \lesssim 500$ GeV, B_q mixings ($q = d, s$) provide the relevant constraint. In particular, and as mentioned before, ρ_{ct} must be turned off⁵³ because of a

ⁿThe $\bar{c}bH^+$ couplings in 2HDM III context has been studied in different decay channels and involving various flavor assumptions,^{113–117} where our list is only partial.

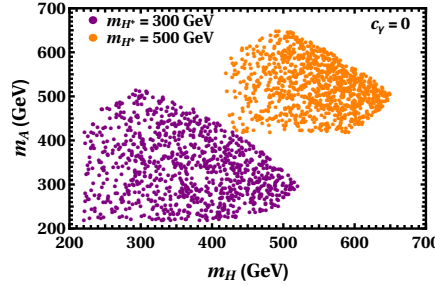


Fig. 7. Scan points in m_H - m_A plane for $c_\gamma = 0$ that pass positivity, perturbativity, unitarity and T parameter constraints.⁶⁹ See text for details.

Table 3. Benchmark point BP1 (BP2) for $m_{H^\pm} = 300$ (500) GeV, with $\eta_6 = 0$ hence $\eta_1 \cong 0.258$ (alignment limit). Higgs masses are in GeV.

	η_2	η_3	η_4	η_5	η_7	μ_{22}^2/v^2	m_{H^\pm}	m_A	m_H
BP1	1.40	0.62	0.53	1.06	-0.79	1.18	300	272	372
BP2	0.71	0.69	1.52	-0.93	0.24	3.78	500	569	517

CKM-enhanced effect in B_q mixings. Assuming all ρ_{ij} vanish except ρ_{tt} , we define $M_{12}^q/M_{12}^q|^{\text{SM}} = C_{B_q}$, with phase negligible. Allowing 2σ error on $C_{B_d} = 1.05 \pm 0.11$ and $C_{B_s} = 1.11 \pm 0.09$ from summer 2018 UTfit,¹²⁶ we give the blue shaded exclusion region in Fig. 8, which extends to upper-right and the left (right) panel is for BP1 (BP2). The constraint from H^+ effects via charm loops¹²⁷ is more forgiving.

$B \rightarrow X_s \gamma$ puts a strong constraint on m_{H^\pm} in 2HDM II, but weakens for g2HDM due to extra Yukawa couplings. An m_t/m_b enhancement factor actually constrains ρ_{bb} more strongly⁵³ than ρ_{tt} . Taking ρ_{bb} as small, the constraint on ρ_{tt} from $B \rightarrow X_s \gamma$ falls outside the range of Fig. 8, while the $B \rightarrow X_s \gamma$ constraint on ρ_{tc} via charm loop is weaker than B_q mixing.⁵³

Overall, because many parameters enter, we view the true constraints from $B \rightarrow X_s \gamma$ on H^+ parameters, e.g. m_{H^\pm} , as still an open issue.

Collider Constraints

For collider constraints, we again set all $\rho_{ij} = 0$ except ρ_{tt} and ρ_{tc} for simplicity. For finite ρ_{tt} , one can have^{128–136} $\bar{b}g \rightarrow \bar{t}(b)H^+$ (our list is not exhaustive), followed by $H^+ \rightarrow t\bar{b}$. Searches at 13 TeV provide model independent bounds on $\sigma(pp \rightarrow \bar{t}(b)H^+) \mathcal{B}(H^+ \rightarrow t\bar{b})$ for $m_{H^\pm} = 200$ GeV to 2 (3) TeV for ATLAS¹¹¹ (CMS¹¹²). Using MadGraph5_aMC@NLO as before with default PDF of NN23LO1 and effective model implemented in FeynRules, we calculate $\sigma(pp \rightarrow \bar{t}(b)H^+) (H^+ \rightarrow t\bar{b})$ at LO for a reference $|\rho_{tt}|$, then rescale by $|\rho_{tt}|^2 \mathcal{B}(H^+ \rightarrow t\bar{b})$ to get the upper limits. For $m_{H^\pm} = 300, 500$ GeV and with $\rho_{tc} = 0$ (hence $\mathcal{B}(H^+ \rightarrow t\bar{b}) \sim 100\%$), we plot the extracted ATLAS (CMS) 95% C.L. bounds on ρ_{tt} as the red (purple) shaded regions in Fig. 8. The ATLAS/CMS limit is more/less stringent than B_q mixing for BP1 while opposite for BP2, with the exclusion bands overlaid to illustrate this.

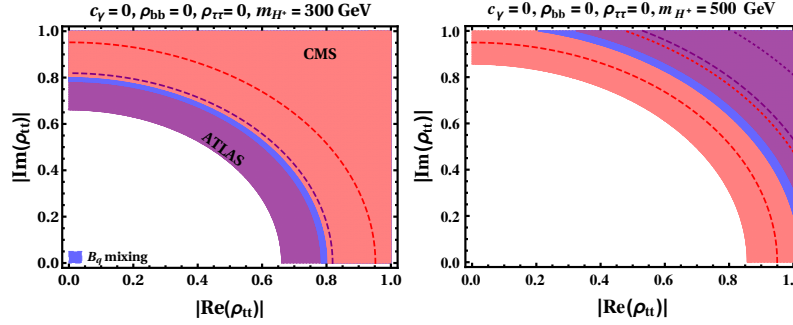


Fig. 8. Constraint from B_q mixings on ρ_{tt} (blue shaded region with area to upper right excluded) assuming all other $\rho_{ij} = 0$. The excluded regions from $bg \rightarrow \bar{t}(b)H^+ \rightarrow \bar{t}(b)t\bar{b}$ searches by ATLAS¹¹¹ and CMS¹¹² for $\rho_{tc} = 0$ are overlaid (purple and red shaded), which is weakened for $\rho_{tc} = 0.4$ (dash) and 0.8 (dots).⁶⁹ See text for details.

Constraints on ρ_{tt} from^{137, 138} $gg \rightarrow H/A \rightarrow t\bar{t}$ search are weaker than results shown in Fig. 8. We will return to the CMS “excess”¹³⁸ at $m_A \sim 400$ GeV later.

The CMS $4t$ search⁷⁶ based on full Run 2 data constrains ρ_{tc} , as discussed in Sec. 4.1.1, but now we consider the constraint together with ρ_{tt} . With both ρ_{tc} and ρ_{tt} finite, the $cg \rightarrow tH/tA \rightarrow t\bar{t}\bar{t}$ process⁶⁸ can feed the SR12 signal region of the CMS $4t$ search if all three top quarks decay semileptonically. As $cg \rightarrow tH/tA \rightarrow t\bar{t}\bar{t}$ barely occurs for BP1 because of low $m_{A,H}$ values, this applies only to BP2. SR12 requires⁷⁶ at least three leptons, four jets with at least three b -tagged, plus p_T^{miss} . We generate events with PYTHIA 6.4 for showering and hadronization, adopt MLM merging^{84, 85} of matrix element and parton shower, then feed into⁸⁶ Delphes 3.4.2 for CMS-based detector card, including b -tagging and c - and light-jet rejection. We find $\rho_{tt} \gtrsim 1$ is excluded if $\rho_{tc} \sim 0.8$ for BP2. However, finite ρ_{tc} induces $H^+ \rightarrow c\bar{b}$ decay, which would dilute $\mathcal{B}(H^+ \rightarrow t\bar{b})$ and soften the $bg \rightarrow \bar{t}(b)H^+$ constraint. This is illustrated by the dash (dot) curves in Fig. 8(right) for $\rho_{tc} = 0.4$ (0.8).

As already discussed in Sec. 4.1.1, the $cg \rightarrow tH/tA \rightarrow t\bar{t}\bar{c}$ process⁶⁸ can feed the CRW control region of CMS $4t$ study when both tops decay semileptonically. Following Refs. 139, 140, we find $\rho_{tc} \gtrsim 0.4$ is excluded for BP1, which is stronger than the B_q mixing bound, and with little dependence on ρ_{tt} . For BP2, CRW gives comparable limit as SR12. Thus, we give in Fig. 8(left) the softened $bg \rightarrow \bar{t}(b)H^+$ constraint only for $\rho_{tc} = 0.4$. Note that analogous searches with similar signature usually involve stronger cuts and therefore do not give relevant constraints.

4.2.2. Collider Signature for $cg \rightarrow bH^+ \rightarrow bt\bar{b}$

We now show that the $cg \rightarrow bH^+ \rightarrow bt\bar{b}$ process, or $pp \rightarrow bH^+ + X \rightarrow bt\bar{b} + X$, is quite promising.⁶⁹ For illustration, we conservatively take $|\rho_{tc}| = 0.4$, $|\rho_{tt}| = 0.6$ for both BPs. Receiving no CKM suppression, the approximate $H^+ \rightarrow c\bar{b}$, $t\bar{b}$ branching ratios are 50%, 50% for BP1, and 36%, 64% for BP2. Assuming $t \rightarrow b\ell\nu_\ell$ ($\ell = e, \mu$), the signature is one charged lepton, p_T^{miss} , and three b -jets. The inclusive

Table 4. Background and signal (Sig, for $\rho_{tc} = 0.4$, $\rho_{tt} = 0.6$) cross sections (in fb) at 14 TeV after selection cuts.

	$t\bar{t}js$	tj	$Wtjs$	$t\bar{t}h$	$t\bar{t}Z$	other	B_{tot}	Sig
BP1	1546	42	27	4.2	1.5	3.1	1627	11.4
BP2	1000	27	16	2.9	1.2	1.9	1049	9.3

final state will receive contributions from $bg \rightarrow \bar{c}H^+ \rightarrow \bar{c}t\bar{b}$ and $bg \rightarrow \bar{t}H^+ \rightarrow \bar{t}c\bar{b}$, as well as ρ_{tt} -induced $bg \rightarrow \bar{t}H^+ \rightarrow \bar{t}t\bar{b}$. Furthermore, the $3b1\ell$ signature will receive mild contributions from $gg \rightarrow \bar{c}bH^+$ and $gg \rightarrow \bar{t}bH^+$ processes. To include such contributions, we have generated $cg \rightarrow bH^+$ events with up to two additional partons, and $bg \rightarrow \bar{t}H^+$ events with one additional parton. The $\bar{c}b \rightarrow H^+ \rightarrow \bar{c}b, \bar{t}b$ processes^o suffer from QCD and top backgrounds for hadronic decay of top, while $\bar{c}b \rightarrow H^+ \rightarrow \bar{t}b$ with semileptonic decay of top is accounted in signal. The dominant backgrounds for $cg \rightarrow bH^+$ arise from $t\bar{t}$ +jets, t - and s -channel single-top (tj), Wt +jets, with subdominant backgrounds from $t\bar{t}h$ and $t\bar{t}Z$. Minor contributions from Drell-Yan and W +jets, $4t$, $t\bar{t}W$, tWh are combined under “other”.

Signal and background samples are generated at LO for 14 TeV as before by MadGraph, interfaced with PYTHIA and fed into Delphes for fast detector simulation adopting default ATLAS-based detector card. The LO $t\bar{t}$ +jets background is normalized to NNLO by a factor⁹⁵ 1.84, and factors of¹⁴¹ 1.2 and 1.47 for t - and s -channel single-top. The LO Wt +jets background is normalized to NLO by a factor¹⁴² 1.35, whereas the subdominant $t\bar{t}h$, $t\bar{t}Z$ receive factors of 1.27,⁹⁴ 1.56.⁹³ The DY+jets background is normalized to NNLO by a factor⁹⁷ 1.27. Finally, the $4t$ and $t\bar{t}W^-$ ($t\bar{t}W^+$) cross sections at LO are adjusted to NLO by factors of 2.04⁸¹ and⁹² 1.35 (1.27). The tWh and W +jets backgrounds are kept at LO. Correction factors for other charge conjugate processes are assumed to be the same, and the signal cross sections are kept at LO.

Events are selected with one lepton with $p_T^\ell > 30$ GeV, at least three jets with three b -tagged and with $p_T^b > 20$ GeV, $|\eta| < 2.5$ for lepton and the b -jets, and $E_T^{\text{miss}} > 35$ GeV. Jets are reconstructed by anti- k_t algorithm using $R = 0.6$. Whether between b -jets or the lepton, we require their $\Delta R > 0.4$. The sum of the lepton and three leading b -jet transverse momenta H_T should be > 350 (400) GeV for BP1 (BP2). The selection cuts for H_T , p_T , E_T^{miss} , etc. are not optimized. The total background B_{tot} (and its various components) and signal Sig cross sections after selection cuts are given in Table 4.

We estimate the statistical significance from Table 4 using Eq. (11). For 137, 300 and 600 fb⁻¹, the significance for $cg \rightarrow bH^+$ is at $\sim 3.3\sigma$, 4.9σ , 6.9σ ($\sim 3.4\sigma$, 5.0σ , 7.1σ) for BP1 (BP2). Reanalyzing for 13 TeV at 137 fb⁻¹, we find similar significance *per* experiment. Thus, full Run 2 data could already show evidence, and combining ATLAS and CMS data is encouraged. Discovery is possible for Run 2+3

^oThe inclusive $\sigma(pp \rightarrow H^+)$ with up to two extra jets in the five flavor scheme for BP1 (BP2) at 14 TeV is 50.8 (6.5) pb using MadGraph5_aMC with NN23LO1 PDF set and default run card.

and beyond. Note that significance can still be high at higher masses for larger ρ_{tc} , ρ_{tt} , but the decoupling μ_{22}^2 would generally become larger,⁵² as can be peeked from $\mu_{22}^2/v^2 \simeq 3.78$ for BP2 in Table 3, which would start to damp the EWBG motivation. The $cg \rightarrow bH^+$ process, however, can certainly be pursued for heavier m_{H^+} at higher luminosities.

Our BPs here involve both ρ_{tc} and ρ_{tt} , and can feed the SS2 ℓ signature. Following the same analysis of Refs. 68 and 139, we find BP1 may have $\sim 3.5\sigma$ significance with full Run 2 data since finite ρ_{tt} plays no effect. But for BP2, the significance is below $\sim 1\sigma$ due to dilution from $A/H \rightarrow t\bar{t}$ decay and falling parton luminosity. Single-top studies may contain $cg \rightarrow bH^+$ events. For $\rho_{tc} = 0.4$ and $\rho_{tt} = 0.6$, we find the combined cross sections for $pp \rightarrow H^+[t\bar{b}]j$, $H^+[c\bar{b}]t$ can contribute 15.2 (2.9) pb for BP1 (BP2), which is within the 2σ error of current t -channel single-top^{143,144} measurements. The situation is similar for Run 1 with s -channel single-top measurements. We have not included uncertainties from scale dependence and PDF, where the latter is sizable for processes initiated by heavy quarks.^{145,146} Using signal cross sections at LO can also bring in some uncertainties, e.g. higher order corrections^{142,147,148} to $\sigma(bg \rightarrow tH^+)$ may amount to 30–40% for $m_{H^+} \sim 300$ –500 GeV. A detailed study of such uncertainties is left for the future, and is part of the reason why we adopt conservative ρ_{tc} , ρ_{tt} values.

5. Discussion and Miscellany

With $\rho_{tt} = \mathcal{O}(\lambda_t) \sim 1$, the heavy Higgs bosons H and A can be produced via gluon-gluon fusion (ggF), and $gg \rightarrow H/A \rightarrow t\bar{t}$ can interfere with the large, QCD-induced $gg \rightarrow t\bar{t}$ amplitude, which distorts the Breit-Wigner peak into a peak-dip structure,¹⁴⁹ making experimental search more challenging. A first study by ATLAS with 8 TeV data starting from 500 GeV found¹³⁷ no significant deviation. Based on 2016 data, CMS reported¹³⁸ more recently an intriguing signal-like deviation in $gg \rightarrow A \rightarrow t\bar{t}$, compatible with an A with mass ~ 400 GeV with global significance of 1.9σ (and 3.5σ local). It was shown¹⁴⁰ that $\rho_{tt} = \mathcal{O}(1)$ can account for this possible “excess”, but $\rho_{tc} = \mathcal{O}(1)$ is called upon to reign in $\mathcal{B}(A \rightarrow t\bar{t})$. It was further pointed out that,¹⁴⁰ for purely imaginary ρ_{tt} — which can robustly drive⁵⁷ EWBG — an H would mimic¹⁵⁰ an A in production and decay, and CMS could well be peeking at the first of the exotic bosons, $m_H \sim 400$ GeV, with heavier, degenerate $m_A \simeq m_{H^+} \gtrsim 550$ GeV satisfying⁵² custodial symmetry, hence more easily fulfill oblique parameter constraints.^p This fits nicely in the range of Eq. (4), and having A – H^+ heavier^q also fits the single-state analysis of CMS.¹³⁸ We eagerly await the unveiling of the full Run 2 data from both CMS and ATLAS.

^pHaving $m_A = 400$ GeV while $m_H \simeq m_{H^+} \gtrsim 550$ GeV would correspond to “twisted” custodial symmetry¹⁵¹ with more restricted parameter space.

^qWe remark that, based on $\sim 36 \text{ fb}^{-1}$, a relatively stringent CMS bound¹⁵² on m_{H^+} from $pp \rightarrow t\bar{t}H^+ + X$ associated production followed by $H^+ \rightarrow t\bar{b}$ would push m_{H^+} beyond 650 GeV. Full Run 2 data, including that from ATLAS, can tell whether this is a downward fluctuation.

But perhaps the excess would disappear with full Run 2 analysis, or some analysis difficulty may be encountered. There is then the $gg \rightarrow H/A \rightarrow t\bar{c}$ process,⁵³ mediated by ρ_{tt} in production and ρ_{tc} in decay. This could be promising, as it does not suffer from interference. However, there is worry⁶⁸ that tj (j stands for a jet) mass resolution¹⁵³ could wash the resonance away. Or one could pursue $H/A \rightarrow \tau\mu$ in the final state, which was shown¹⁵⁴ to hold promise at the HL-LHC, but would likely suffer from suppressed $\mathcal{B}(H/A \rightarrow \tau\mu)$, as $\rho_{\tau\mu} = \mathcal{O}(\lambda_\tau) \sim 0.01$ would be our best guess.¹⁵⁵ In principle, $H/A \rightarrow \tau\tau$ can also be searched for, but there is no “large $\tan\beta$ ” enhancement mechanism as in 2HDM II, where again our best guess would be $\rho_{\tau\tau} = \mathcal{O}(\lambda_\tau)$ in g2HDM, that the second diagonal τ Yukawa coupling should go with the strength of λ_τ by the mass-mixing hierarchy argument. We note the prowess of ATLAS¹⁵⁶ and CMS¹⁵⁷ with simple final states containing τ s.

This brings us back to our main proposed processes of $cg \rightarrow tH/A \rightarrow t\bar{t}\bar{c}$, $t\bar{t}$ and $cg \rightarrow bH^+ \rightarrow b\bar{t}\bar{b}$, but turning to the ρ_{tu} -induced process. Although $\rho_{tu} < \rho_{tc}$ is expected by way of mass-mixing argument, this is not based on direct experimental knowledge. In Sec. 4.1.1., we followed Ref. 80 to study the effect of CRW of CMS $4t$ analysis and CRttW2 ℓ of ATLAS $4t$ analysis on ρ_{tu} , and plotted the results in Fig. 4[right]. The bounds from $4t$ analyses on ρ_{tu} are indeed more stringent than on ρ_{tc} of Fig. 4[left], but by far not as stringent by a $\sqrt{m_u/m_c}$ factor as implied roughly by the mass-mixing hierarchy. Furthermore, these bounds were studied keeping⁸⁰ $\rho_{tu} \neq 0$ but setting all other $\rho_{ij} = 0$, with exclusion limits and discovery reach also plotted in Fig. 4[right]. If ρ_{tu} and ρ_{tc} are both kept,⁸⁰ given that there are no good tools for separating c - and light q -jets, it would not be easy to gain on extracting information. We note, therefore, that the product $\rho_{tu}\rho_{\tau\mu}$ would be probed by¹¹⁸ the $B \rightarrow \mu\nu$ process at Belle II. If any deviation¹⁵⁸ of $\mathcal{B}(B \rightarrow \mu\nu)/\mathcal{B}(B \rightarrow \tau\nu)$ from SM expectation is observed, it would imply that both ρ_{tu} and $\rho_{\tau\mu}$ are nonvanishing, and more sophisticated analysis for having ρ_{tu} and ρ_{tc} both finite need to be developed, where Ref. 80 is only a start. The $\rho_{\tau\mu}$ coupling can also be probed via the $\tau \rightarrow \mu\gamma$ process^{155,159} at Belle II with the help of ρ_{tt} via the two-loop mechanism.¹⁶⁰ Thus, there is much synergies with the flavor frontier to look forward to, and with refined analyses at the (HL-)LHC, much progress can be anticipated.

Finally, let us comment on the implications of finite c_γ . For exotic Higgs in the mass range of Eq. (4), in general one would expect h - H mixing, i.e. c_γ , to be finite. However, compared with the $\cos(\beta - \alpha)$ fit to Higgs property measurements^{161,162} at the LHC in 2HDM II (which is implied by SUSY), the many more parameters that can enter for production and decay of the h boson, as we have illustrated only partially, implies that a similar fit to c_γ (the equivalent to $\cos(\beta - \alpha)$) seems nowhere in sight. We can only argue that c_γ has to be small to have h resembling the Higgs boson of SM so well, but its value is not known.

With c_γ small but nonzero, what could be the implications? The H and A (and H^+) would become mildly related to electroweak symmetry breaking, e.g. coupling to W and Z bosons. We mention here only a few collider possibilities. The first would be resonant di-Higgs production via the $cg \rightarrow tH \rightarrow thh$ process,

where a finite c_γ induces an effective λ_{Hhh} coupling.¹²⁵ This can be searched for at the LHC via $pp \rightarrow tH + X \rightarrow thh + X$, and non-negligible discovery potential is found¹²⁵ at the LHC for $m_H \lesssim 350$ GeV and $\rho_{tc} \gtrsim 0.5$. A second process would be $cg \rightarrow tA \rightarrow tZH$,¹⁶³ where sufficient m_A - m_H splitting is required to allow for $A \rightarrow ZH$ decay. It further requires ρ_{tt} to be small, otherwise $A \rightarrow t\bar{t}$ would in general be too strong. Under these conditions, it is found¹⁶³ that discovery is possible at the HL-LHC for $m_A \sim 400$ GeV, hence $m_H \lesssim 300$ GeV, but tZh production is not promising. A third example, discussed recently,¹⁶⁴ targets the conclusive investigation of the ρ_{tc} mechanism⁵⁷ for EWBG (in the case that ρ_{tt} turns out small), which can more easily⁶⁰ survive the eEDM constraint as ρ_{tc} does not enter the Barr-Zee two-loop mechanism. The ρ_{tc} mechanism requires $\rho_{tc} \gtrsim 0.5$. The proposal¹⁶⁴ is to utilize $cg \rightarrow bH^+ \rightarrow bW^+h$ for $c_\gamma \gtrsim 0.1$ to efficiently push the ρ_{tc} bound (or discovery!) down to 0.2 or below at the HL-LHC. For small $c_\gamma \lesssim 0.12$, one counts on the $cg \rightarrow tH/A \rightarrow t\bar{t}\bar{c}$ process, which depends rather weakly on c_γ , to push the exclusion (or discovery!) down to 0.25 or below. Combined, this two-prong search can draw a conclusion on the ρ_{tc} mechanism.

6. Summary and Prospect

In the past few years, we have verified the Yukawa couplings of t , b quarks and τ , μ charged leptons, making extra Yukawa couplings involving a second Higgs doublet plausible and attractive. This general 2HDM with extra Yukawa couplings point to extra Higgs bosons H , A and H^+ in the sub-TeV range, which is based on naturalness of the second set of dimension-4 couplings unique to the Higgs sector: Higgs quartic self-couplings. The exotic bosons are well hidden so far by fermion mass-mixing hierarchy and alignment, the smallness of h - H mixing angle c_γ .

The search for $t \rightarrow ch$ (and concurrently for $h \rightarrow \tau\mu$) is ongoing. If it does not emerge with full Run 2 data, it would constrain the product of $\rho_{tc} c_\gamma$. But given that c_γ is small, sizable ρ_{tc} would still be allowed. In this brief review, we advocate the search for $cg \rightarrow tH/A \rightarrow t\bar{t}\bar{c}$, $t\bar{t}\bar{t}$ and $cg \rightarrow bH^+ \rightarrow b\bar{t}\bar{b}$ at the LHC, where production, unhampered by small c_γ , depends on sizable ρ_{tc} , while the $t\bar{t}\bar{t}$ and $b\bar{t}\bar{b}$ final states require finite ρ_{tt} for $H/A \rightarrow t\bar{t}$ and $H^+ \rightarrow t\bar{b}$ decays. It would be interesting, therefore, to follow up with full Run 2 data on the $m_A \sim 400$ GeV excess seen by CMS in $t\bar{t}$ resonance search. Both extra top Yukawa couplings ρ_{tt} and ρ_{tc} can drive electroweak baryogenesis, providing further impetus for search. LHC Run 2 data may already be promising, and Run 2+3 data would be even more revealing, while HL-LHC may hold the ultimate promise for discovery, which would open up a new chapter at the intersection of Higgs and flavor physics.

Acknowledgments

WSH is supported by MOST 109-2112-M-002-015-MY3 of Taiwan and NTU 109L104019. TM is supported by a Postdoctoral Research Fellowship from Alexander von Humboldt Foundation.

References

1. W.-S. Hou, Phys. Lett. B **296**, 179 (1992).
2. T.P. Cheng and M. Sher, Phys. Rev. D **35**, 3484 (1987).
3. S.L. Glashow and S. Weinberg, Phys. Rev. D **15**, 1958 (1977).
4. L.J. Hall and S. Weinberg, Phys. Rev. D **48**, R979 (1993).
5. W.-S. Hou, Phys. Rev. Lett. **72**, 3945 (1994).
6. G.C. Branco *et al.*, Phys. Rept. **516**, 1 (2012).
7. G. Aad *et al.* [ATLAS and CMS], JHEP **08**, 045 (2016).
8. P.A. Zyla *et al.* [PDG], PTEP **2020**, 083C01 (2020).
9. D. Atwood, L. Reina and A. Soni, Phys. Rev. D **53**, 1199 (1996).
10. W.-S. Hou and G.-L. Lin, Phys. Lett. B **379**, 261 (1996).
11. S. Bar-Shalom, G. Eilam, A. Soni and J. Wudka, Phys. Rev. Lett. **79**, 1217 (1997).
12. W.-S. Hou, G.-L. Lin and C.-Y. Ma, Phys. Rev. D **56**, 7434 (1997).
13. S. Bar-Shalom, G. Eilam, A. Soni and J. Wudka, Phys. Rev. D **57**, 2957 (1998).
14. S. Bar-Shalom and J. Wudka, Phys. Rev. D **60**, 094016 (1999).
15. T. Han, J. Jiang and M. Sher, Phys. Lett. B **516**, 337 (2001).
16. Y. Jiang *et al.*, Phys. Rev. D **57**, 4343 (1998).
17. D. Atwood, L. Reina and A. Soni, Phys. Rev. Lett. **75**, 3800 (1995).
18. W.-S. Hou, G.-L. Lin, C.-Y. Ma and C.-P. Yuan, Phys. Lett. B **409**, 344 (1997).
19. D. Atwood, L. Reina and A. Soni, Phys. Rev. D **55**, 3156 (1997).
20. J.A. Aguilar-Saavedra, Acta Phys. Polon. B **35**, 2695 (2004).
21. G. Eilam, J.L. Hewett and A. Soni, Phys. Rev. D **44**, 1473 (1991) Erratum: [Phys. Rev. D **59**, 039901 (1999)].
22. B. Mele, S. Petrarca and A. Soddu, Phys. Lett. B **435**, 401 (1998).
23. T. Han and R. Ruiz, Phys. Rev. D **89**, 074045 (2014).
24. See e.g. S. Béjar, J. Guasch and J. Solà, Nucl. Phys. B **600**, 21 (2001).
25. A. Arhrib, Phys. Rev. D **72**, 075016 (2005).
26. I. Baum, G. Eilam and S. Bar-Shalom, Phys. Rev. D **77**, 113008 (2008).
27. A.K. Das and C. Kao, Phys. Lett. B **372**, 106 (1996).
28. See e.g. J. Guasch and J. Solà, Nucl. Phys. B **562**, 3 (1999).
29. J.-J. Cao *et al.*, Phys. Rev. D **75**, 075021 (2007).
30. J. Cao, C. Han, L. Wu, J.-M. Yang and M. Zhang, Eur. Phys. J. C **74**, 3058 (2014).
31. G. Eilam *et al.*, Phys. Lett. B **510**, 227 (2001).
32. J.A. Aguilar-Saavedra, Phys. Rev. D **67**, 035003 (2003).
33. R. Gaitán, O.G. Miranda and L.G. Cabral-Rosetti, Phys. Rev. D **72**, 034018 (2005).
34. A. Azatov, M. Toharia and L. Zhu, Phys. Rev. D **80**, 035016 (2009).
35. B. Yang, N. Liu and J. Han, Phys. Rev. D **89**, 034020 (2014).
36. A. Azatov, G. Panico, G. Perez and Y. Soreq, JHEP **1412**, 082 (2014).
37. G. Abbas, A. Celis, X.-Q. Li, J. Lu and A. Pich, JHEP **1506**, 005 (2015).
38. J.A. Aguilar-Saavedra and G.C. Branco, Phys. Lett. B **495**, 347 (2000).
39. E.O. Iltan, Phys. Rev. D **65**, 075017 (2002).
40. J.I. Aranda, A. Cordero-Cid, F. Ramírez-Zavaleta, J.J. Toscano and E.S. Tututi, Phys. Rev. D **81**, 077701 (2010).
41. A. Cordero-Cid, M.A. Pérez, G. Tavares-Velasco and J.J. Toscano, Phys. Rev. D **70**, 074003 (2004).
42. F. Larios, R. Martínez and M.A. Pérez, Phys. Rev. D **72**, 057504 (2005).
43. A. Fernández, C. Pagliarone, F. Ramírez-Zavaleta and J.J. Toscano, J. Phys. G **37**, 085007 (2010).
44. C. Kao, H.-Y. Cheng, W.-S. Hou and J. Sayre, Phys. Lett. B **716**, 225 (2012).
45. K.-F. Chen, W.-S. Hou, C. Kao and M. Kohda, Phys. Lett. B **725**, 378 (2013).

46. V. Khachatryan *et al.* [CMS], Phys. Lett. B **749**, 337 (2015).
47. C.-W. Chiang, H. Fukuda, M. Takeuchi and T.T. Yanagida, JHEP **1511**, 057 (2015).
48. A. Crivellin, J. Heeck and P. Stoffer, Phys. Rev. Lett. **116**, 081801 (2016).
49. F.J. Botella, G.C. Branco, M. Nebot and M.N. Rebelo, Eur. Phys. J. C **76**, 161 (2016).
50. C.-W. Chiang, H. Fukuda, M. Takeuchi and T.T. Yanagida, Phys. Rev. D **97**, 035015 (2018).
51. See e.g. S. Davidson and H.E. Haber, Phys. Rev. D **72**, 035004 (2005).
52. W.-S. Hou and M. Kikuchi, EPL **123**, 11001 (2018).
53. B. Altunkaynak, W.-S. Hou, C. Kao, M. Kohda and B. McCoy, Phys. Lett. B **751**, 135 (2015).
54. F. Mahmoudi and O. Stål, Phys. Rev. D **81**, 035016 (2010).
55. A.M. Sirunyan *et al.* [CMS], Phys. Rev. Lett. **120**, 231801 (2018).
56. M. Aaboud *et al.* [ATLAS], Phys. Lett. B **784**, 173 (2018).
57. K. Fuyuto, W.-S. Hou and E. Senaha, Phys. Lett. B **776**, 402 (2018).
58. See e.g. S. Kanemura, Y. Okada and E. Senaha, Phys. Lett. B **606**, 361 (2005).
59. V. Andreev *et al.* [ACME], Nature **562**, 355 (2018).
60. K. Fuyuto, W.-S. Hou and E. Senaha, Phys. Rev. D **101**, 011901(R) (2020).
61. N. Craig *et al.*, Phys. Rev. D **86**, 075002 (2012).
62. S. Chatrchyan *et al.* [CMS], JHEP **1206**, 169 (2012).
63. The ATLAS collaboration, ATLAS-CONF-2013-081.
64. G. Aad *et al.* [ATLAS], JHEP **1406**, 008 (2014).
65. V. Khachatryan *et al.* [CMS], Phys. Rev. D **90**, 112013 (2014).
66. M. Aaboud *et al.* [ATLAS], JHEP **1905**, 123 (2019).
67. M. Aaboud *et al.* [ATLAS], JHEP **1710**, 129 (2017).
68. M. Kohda, T. Modak and W.-S. Hou, Phys. Lett. B **776**, 379 (2018).
69. D.K. Ghosh, W.-S. Hou and T. Modak, Phys. Rev. Lett. **125**, 221801 (2020).
70. E.L. Berger, Q.-H. Cao, C.-R. Chen, C.S. Li and H. Zhang, Phys. Rev. Lett. **106**, 201801 (2011).
71. G. Aad *et al.* [ATLAS Collaboration], JHEP **1204**, 069 (2012).
72. S. Chatrchyan *et al.* [CMS Collaboration], JHEP **1208**, 110 (2012).
73. J. Ebadi, F. Elahi, M. Khatiri and M. Mohammadi Najafabadi, Phys. Rev. D **98**, 075012 (2018).
74. S. Cho, P. Ko, J. Lee, Y. Omura and C. Yu, Phys. Rev. D **101**, 055015 (2020).
75. V. Barger, W.-Y. Keung and B. Yencho, Phys. Lett. B **687**, 70 (2010).
76. A.M. Sirunyan *et al.* [CMS], Eur. Phys. J. C **80**, 75 (2020).
77. G. Aad *et al.* [ATLAS], Eur. Phys. J. C **80**, 1085 (2020).
78. R. Frederix, D. Pagani and M. Zaro, JHEP **1802**, 031 (2018); and references therein.
79. The process was discussed by S. Gori, C. Grojean, A. Juste and A. Paul, JHEP **1801**, 108 (2018), without detailed study.
80. W.-S. Hou, T.-H. Hsu and T. Modak, Phys. Rev. D **102**, 055006 (2020).
81. J. Alwall *et al.*, JHEP **1407**, 079 (2014).
82. R.D. Ball *et al.* [NNPDF], Nucl. Phys. B **877**, 290 (2013).
83. T. Sjöstrand, S. Mrenna and P. Skands, JHEP **0605**, 026 (2006).
84. M.L. Mangano, M. Moretti, F. Piccinini and M. Treccani, JHEP **0701**, 013 (2007).
85. J. Alwall *et al.*, Eur. Phys. J. C **53**, 473 (2008).
86. J. de Favereau *et al.* [DELPHES 3], JHEP **1402**, 057 (2014).
87. A. Alloul *et al.*, Comput. Phys. Commun. **185**, 2250 (2014).
88. W.-S. Hou, M. Kohda and T. Modak, Phys. Rev. D **98**, 015002 (2018).
89. The ATLAS Collaboration, ATLAS-CONF-2016-037.
90. E. Alvarez, D.A. Faroughy, J.F. Kamenik, R. Morales and A. Szykman, Nucl. Phys.

- B **915**, 19 (2017).
91. M. Aaboud *et al.* [ATLAS], JHEP **1812**, 039 (2018).
 92. J.M. Campbell and R.K. Ellis, JHEP **1207**, 052 (2012).
 93. J. Campbell, R.K. Ellis and R. Röntsch, Phys. Rev. D **87**, 114006 (2013).
 94. SM Higgs production cross sections at $\sqrt{s} = 14$ TeV, <https://twiki.cern.ch/twiki/bin/view/LHCPhysics/CERNYellowReportPageAt14TeV2010>.
 95. ATLAS-CMS recommended $t\bar{t}$ cross section predictions, <https://twiki.cern.ch/twiki/bin/view/LHCPhysics/TtbarNNLO>.
 96. W.-S. Hou, M. Kohda and T. Modak, Phys. Rev. D **96**, 015037 (2017).
 97. Y. Li and F. Petriello, Phys. Rev. D **86**, 094034 (2012).
 98. A.M. Sirunyan *et al.* [CMS Collaboration], Eur. Phys. J. C **77**, 578 (2017).
 99. G. Cowan, K. Cranmer, E. Gross and O. Vitells, Eur. Phys. J. C **71**, 1554 (2011).
 100. A.M. Sirunyan *et al.* [CMS], Eur. Phys. J. C **80**, 752 (2020).
 101. C. Han, N. Liu, L. Wu and J.M. Yang, Phys. Lett. B **714**, 295 (2012).
 102. S. Kanemura, H. Yokoya and Y.-J. Zheng, Nucl. Phys. B **898**, 286 (2015).
 103. R. Patrick, P. Sharma and A.G. Williams, Phys. Lett. B **780**, 603 (2018).
 104. M. Malekhosseini, M. Ghominejad, H. Khanpour and M. Mohammadi Najafabadi, Phys. Rev. D **98**, 095001 (2018).
 105. H. Khanpour, Nucl. Phys. B **958**, 115141 (2020).
 106. C.-R. Chen, Phys. Lett. B **736**, 321 (2014).
 107. Q.-H. Cao, S.-L. Chen, Y. Liu and X.-P. Wang, Phys. Rev. D **100**, 055035 (2019).
 108. S. Khatibi and H. Khanpour, arXiv:2011.15060 [hep-ph].
 109. The CMS Collaboration, CMS-PAS-TOP-17-005.
 110. G. Aad *et al.* [ATLAS], Eur. Phys. J. C **76**, 259 (2016).
 111. M. Aaboud *et al.* [ATLAS], JHEP **1811**, 085 (2018).
 112. A.M. Sirunyan *et al.* [CMS], JHEP **2001**, 096 (2020).
 113. H.-J. He and C.-P. Yuan, Phys. Rev. Lett. **83**, 28 (1999).
 114. J.L. Diaz-Cruz, J. Hernández-Sánchez, S. Moretti, R. Noriega-Papaqui and A. Rosado, Phys. Rev. D **79**, 095025 (2009).
 115. J. Hernández-Sánchez, S. Moretti, R. Noriega-Papaqui and A. Rosado, JHEP **1307**, 044 (2013).
 116. O. Flores-Sánchez, J. Hernández-Sánchez, C.G. Honorato, S. Moretti and S. Rosado-Navarro, Phys. Rev. D **99**, 095009 (2019).
 117. J. Hernández-Sánchez, C.G. Honorato, S. Moretti and S. Rosado-Navarro, Phys. Rev. D **102**, 055008 (2020).
 118. W.-S. Hou, M. Kohda, T. Modak and G.-G. Wong, Phys. Lett. B **800**, 135105 (2020).
 119. S. Iguro and K. Tobe, Nucl. Phys. B **925**, 560 (2017).
 120. U. Nierste, M. Tabet and R. Ziegler, Phys. Rev. Lett. **125**, 031801 (2020).
 121. D. Eriksson, J. Rathsmann and O. Stål, Comput. Phys. Commun. **181**, 189 (2010).
 122. Taken from http://project-gfitter.web.cern.ch/project-gfitter/Oblique_Parameters/.
 123. C.D. Froggatt, R.G. Moorhouse and I.G. Knowles, Phys. Rev. D **45**, 2471 (1992).
 124. H.E. Haber and O. Stål, Eur. Phys. J. C **75**, 491 (2015).
 125. W.-S. Hou, M. Kohda and T. Modak, Phys. Rev. D **99**, 055046 (2019).
 126. See <http://www.utfit.org/UTfit/ResultsSummer2018NP>.
 127. A. Crivellin, A. Kokulu and C. Greub, Phys. Rev. D **87**, 094031 (2013).
 128. J.F. Gunion, H.E. Haber, F.E. Paige, W.-K. Tung and S.S.D. Willenbrock, Nucl. Phys. B **294**, 621 (1987).
 129. J.L. Diaz-Cruz and O.A. Sampayo, Phys. Rev. D **50**, 6820 (1994).
 130. S. Moretti and D.P. Roy, Phys. Lett. B **470**, 209 (1999).
 131. D.J. Miller, S. Moretti, D.P. Roy and W.J. Stirling, Phys. Rev. D **61**, 055011 (2000).

132. A. Arhrib, R. Benbrik, H. Harouiz, S. Moretti and A. Rouchad, *Front. Phys.*, 10 March 2020 doi:10.3389/fphy.2020.00039.
133. A. Arhrib *et al.*, *JHEP* **2010**, 209 (2020).
134. J.-Y. Cen, J.-H. Chen, X.-G. He, G. Li, J.-Y. Su and W. Wang, *JHEP* **1901**, 148 (2019).
135. P. Sanyal, *Eur. Phys. J. C* **79**, 913 (2019).
136. B. Coleppa, A. Sarkar and S.K. Rai, *Phys. Rev. D* **101**, 055030 (2020).
137. M. Aaboud *et al.* [ATLAS], *Phys. Rev. Lett.* **119**, 191803 (2017).
138. A.M. Sirunyan *et al.* [CMS], *JHEP* **04**, 171 (2020).
139. W.-S. Hou, M. Kohda and T. Modak, *Phys. Lett. B* **786**, 212 (2018).
140. W.-S. Hou, M. Kohda and T. Modak, *Phys. Lett. B* **798**, 134953 (2019).
141. ATLAS-CMS recommended predictions for single-top cross sections using the Hathor v2.1 program, <https://twiki.cern.ch/twiki/bin/view/LHCPhysics/SingleTopRefXsec>.
142. N. Kidonakis, *Phys. Rev. D* **82**, 054018 (2010).
143. M. Aaboud *et al.* [ATLAS], *JHEP* **1704**, 086 (2017).
144. A.M. Sirunyan *et al.* [CMS], *Phys. Lett. B* **800**, 135042 (2020).
145. M. Buza Y. Matiounine, J. Smith and W.L. van Neerven, *Eur. Phys. J. C* **1**, 301 (1998).
146. F. Maltoni, G. Ridolfi and M. Ubiali, *JHEP* **1207**, 022 (2012).
147. T. Plehn, *Phys. Rev. D* **67**, 014018 (2003).
148. E.L. Berger, T. Han, J. Jiang and T. Plehn, *Phys. Rev. D* **71**, 115012 (2005).
149. For a recent discussion, see M. Carena and Z. Liu, *JHEP* **1611**, 159 (2016).
150. For illustration with $\rho_{tt} c_\gamma$ coupling in $gg \rightarrow h \rightarrow t\bar{t}$, see W.-S. Hou, M. Kohda and T. Modak, *Phys. Rev. D* **98** 075007 (2018).
151. J.-M. Gérard and M. Herquet, *Phys. Rev. Lett.* **98**, 251802 (2007).
152. A.M. Sirunyan *et al.* [CMS], *JHEP* **2007**, 126 (2020).
153. See e.g. A.M. Sirunyan *et al.* [CMS], *Phys. Lett. B* **778**, 349 (2018).
154. W.-S. Hou, R. Jain, C. Kao, M. Kohda, B. McCoy and A. Soni, *Phys. Lett. B* **795**, 371 (2019).
155. W.-S. Hou and G. Kumar, arXiv:2008.08469 [hep-ph].
156. See e.g. G. Aad *et al.* [ATLAS], *Phys. Rev. Lett.* **125**, 051801 (2020).
157. See e.g. A.M. Sirunyan *et al.* [CMS], *JHEP* **2003**, 103 (2020).
158. P. Chang, K.-F. Chen and W.-S. Hou, *Prog. Part. Nucl. Phys.* **97**, 261 (2017).
159. W.-S. Hou and G. Kumar, *Phys. Rev. D* **101**, 095017 (2020).
160. D. Chang, W.-S. Hou and W.-Y. Keung, *Phys. Rev. D* **48**, 217 (1993).
161. For the most recent, see A.M. Sirunyan *et al.* [CMS], *Eur. Phys. J. C* **79**, 421 (2019).
162. For the most recent, see G. Aad *et al.* [ATLAS], *Phys. Rev. D* **101**, 012002 (2020).
163. W.-S. Hou and T. Modak, *Phys. Rev. D* **101**, 035007 (2020).
164. W.-S. Hou, T. Modak and T. Plehn, arXiv:2012.03572 [hep-ph].